Rapid and reversible changes in intrahippocampal connectivity during the course of hibernation in European hamsters

Ana María Magariños*†, Bruce S. McEwen*†, Michel Saboureau‡, and Paul Pevet‡

*The Rockefeller University, 1230 York Avenue, New York, NY 10021; and ‡Institut des Neurosciences Cellulaires et Intégratives LC2 7168, Centre National de la Recherche Scientifique-Universite Louis Pasteur, F-67085 Strasbourg, France

Contributed by Bruce S. McEwen, October 5, 2006 (sent for review June 1, 2006)

The hippocampal formation is a highly plastic brain structure that undergoes structural remodeling in response to internal and external challenges such as metabolic imbalance and repeated stress. We investigated whether the extreme alterations in metabolic status that occur during the course of hibernation in European hamsters cause structural changes in the dendritic arborizations of the CA3 pyramidal neurons and their main excitatory afferents, the mossy fiber terminals (MFT), that originate in the dentate gyrus. We report that apical, but not basal, dendritic trees of Golgi-impregnated CA3 principal neurons are significantly shorter, less branched, and less spiny in hypothermic hamsters compared with active animals. After the induction of arousal from torpor, within 2 h, the apical dendritic lengths, branching patterns, and spine density estimations returned to levels found in active, euthermic hamsters. The ultrastructure of MFT in hibernating hamsters showed a significant reduction in synaptic vesicle density and in the percentage of MFT area covered by spine profiles. Awakened hamsters showed restoration of MFT morphology to that seen in active animals. MFT of torpid animals also showed a significant increase in the percentage area of mitochondrial profiles that remained higher 3 h after induced arousal from hibernation compared with euthermic controls. Thus, the torpid/awakening cycle of the hibernating European hamster causes a rapid and reversible morphological reorganization of intrahippocampal subregions involved in information processing. The reported reductions in morphological connectivity between the dentate gyrus and the CA3 subregions could underlie the cessation of exploratory activity and spatial navigation skills during hibernation.

CA3 region | hippocampus | mossy fibers | spines | Golgi impregnation

Hibernation is a highly regulated physiological response to adverse environmental conditions characterized by hypothermia and drastic reductions of metabolic rate (1). Hibernating species can adapt to anticipated scarcity in food supply and decreases in ambient temperature by storing food and increasing food intake for several weeks before winter starts (2). Once the animals enter into hibernation, they develop an energy conserving behavior and undergo deep bouts of hypothermia (or torpor) alternated with short euthermic intervals termed periodic arousals (3). By using fat stores as their primary source of energy and reducing carbohydrate metabolism, hibernating mammals sustain vital functions during prolonged periods without feeding and support periodic rewarming during interbout arousals (4).

The physiological mechanisms triggering hibernation are very complex and far from being well known. Its seasonal occurrence is primarily regulated by the annual photoperiodic variations, and the neuroendocrine and neural mechanisms involved have been partly identified (5–8). The hippocampus, a target brain region for stressful challenges and adrenal steroids (9), has been postulated as a key structure in the hibernation/awakening cycle, especially during arousal (10). In fact, the hippocampus, among other limbic structures, displays continuous EEG activity throughout the hibernation bout and is one of the first brain structures to regain its normal electrical activity before the arousal process begins (11). These observations contrast with the relative electrical silence in cortical and midbrain areas during hibernation and underscore the subordination of the reappearance of their electrical activity to hippocampal control (3, 12). A complex structural connectivity within the hippocampus mediates spatial behaviors such as the storage and retrieval of food stores by birds and mammals within their defined territory (13, 14). Stressful challenges can affect the structural connectivity and, ultimately, the function of the hippocampal formation. We have reported that repeated stress causes rat hippocampal neurons to undergo structural remodeling, particularly at the junction between the mossy fiber input from the dentate gyrus and the CA3 pyramidal neurons (15). Hibernation represents an interesting example of rapid and profound changes in brain metabolism during which the torpid animal becomes disengaged from its normal daily activity involving food seeking, storage, and retrieval to minimize energy expenditure. We tested the hypothesis that during the hibernation cycle of European hamsters, an experimental model in which the characteristics of the hibernation cycle are well defined (8), the hippocampal mediation of spatial memory processing and exploratory activity is temporarily disengaged, and this ''disuse'' has a structural substrate in the hippocampus. In addition, because hibernators have the ability to spontaneously restore the euthermic state in a short period, they provide a unique model to investigate, under physiological conditions, the reversible effects of drastic changes in cell activity on brain structure.

Results

Effects of Hibernation and Induced Awakening on the Structure of the Hippocampus. The morphometric analysis of Golgi-impregnated hippocampal sections revealed that CA3 principal neurons of hibernating hamsters have a reduced complexity of their apical dendritic arborizations as indicated by the decreased number of branch points and the reduction in total dendritic length compared with active controls (Fig. 1). The apical dendritic retraction was readily reversible, because 2 h after the induction of arousal, apical dendrites were more branched and longer than in torpid hamsters, reaching the levels of branching complexity observed in active hamsters. No further changes were detected 3 h after the artificially provoked arousal in the number of bifurcations and total length of the apical dendritic arborizations (Fig. 1). Whereas the apical dendritic fields of CA3 pyramidal

Author contributions: A.M.M., B.S.M., M.S., and P.P. designed research; A.M.M., B.S.M., M.S., and P.P. performed research; A.M.M., B.S.M., M.S., and P.P. contributed new reagents/analytic tools; A.M.M., B.S.M., M.S., and P.P. analyzed data; and A.M.M., B.S.M., M.S., and P.P. wrote the paper.

The authors declare no conflict of interest.

Abbreviation: MFT, mossy fiber terminals.

†To whom correspondence may be addressed. E-mail: magaria@mail.rockefeller.edu or mcewen@rockefeller.edu.

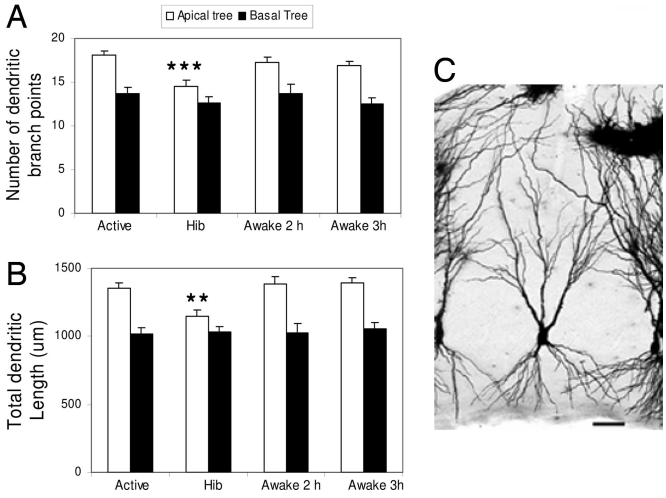

Fig. 1. Deep hibernation affects dendritic morphology of CA3 pyramidal neurons. (*A* and *B*) Effect of deep hibernation (Hib) and induced awakening (Awake 2 and 3 h) on the number of dendritic branch points (*A*) and total dendritic length (*B*) of pyramidal neurons from hippocampal CA3 subregion. (*C*) A representative Golgi stained CA3 pyramidal cell. The image was captured on a Zeiss Axioplan 2i microscope fitted with a Plan Neofluar ×10/0.3 N.A. objective lens and a Hamamatsu Orca ER cooled CCD camera by using MetaVue acquisition software. A stack of 24 images was captured at 2-μm intervals, and the image was displayed as an average projection. (Scale bar: 50 μm.) ** and *** are $P < 0.05$ and $P < 0.001$, respectively, compared with active controls. One-way ANOVA, Tukey post hoc test. Bars represent means plus SEM.

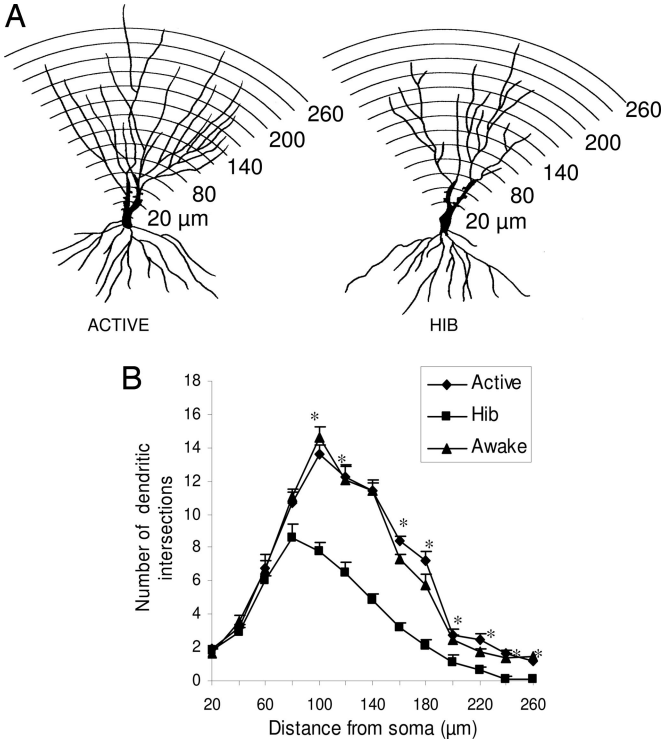

Fig. 2. Effect of deep hibernation and induced awakening on the apical dendritic branching density of CA3 pyramidal neurons. (*A*) Camera lucida drawings of representative CA3 pyramidal neurons from active and hibernating European hamsters. An overlay of concentric rings centered at the cell body was used for Sholl analysis. (*B*) One-way ANOVA followed by Tukey post hoc test revealed statistical differences among experimental groups between 100 and 180 μm from the soma [hibernation (HIB) vs. active and awaken groups, $P < 0.001$) and also between 200 and 260 μm from the soma [HIB vs. active and awaken groups ($P < 0.005$)].

neurons showed significant and reversible plastic changes in response to hibernation, the length and number of branch points of the basal dendritic trees were unaffected and remained stable throughout the torpor/arousal cycle. No significant changes were observed in the apical and basal dendritic architecture of pyramidal neurons from extrahippocampal brain areas such as layer V of the parietal cortex across the hibernation cycle (Fig. 5, which is published as supporting information on the PNAS web site). To further investigate the structural changes induced by hibernation, we estimated the dendritic branching densities of the apical dendritic trees of CA3 pyramidal neurons. Scholl analysis revealed that hibernating hamsters show reduced dendritic material compared with active and awakened ones (Fig. 2). This effect was observed in the outer two-thirds of the apical dendritic trees containing quaternary and higher-order dendritic segments (Fig. 2). Contrarily, the proximal third of the dendritic arborization where primary, secondary, and tertiary dendritic order prevail showed no differences in branching density among experimental groups (Fig. 2). During deep hypothermia, spine density of CA3 pyramidal apical dendrites decreased compared with nonhibernating controls and returned to levels found in euthermic hamsters after inducing awakening. No variations in spine density were detected during the hibernation cycle in CA1 pyramidal neurons (Fig. 6, which is published as supporting information on the PNAS web site).

Toluidine blue staining of semithin sections containing the hippocampal CA3 subregion revealed that hibernation causes specific morphological changes within the stratum pyramidale. The majority of the cell bodies from hamsters in deep hypothermia contained characteristic fissures or "slits" that ranged between 4.5 and 13 μm in length and 0.4 and 1.5 μm in width and appear to be associated with enlarged or distended endoplasmic reticulum membranes. Within the cell bodies, the nuclear envelope of CA3 pyramidal neurons is associated with multiple and profound invaginations in hibernating hamsters (Fig. 3).

Hibernation Causes a Reversible Ultrastructural Reorganization of MFT and Giant Spines of CA3 Pyramidal Neurons. The quantitative morphometry of the MFT and their postsynaptic elements, the giant CA3 spines, revealed that the area of MFT relative to the stratum lucidum area examined did not differ among experimental groups (Table 1). During the hibernation cycle, a reversible decrease was detected in the percentage area of MFT occupied by giant spine profiles with decreases observed during deep torpor. This postsynaptic reorganization induced by deep hypothermia was readily reversible and only 3 h after the induction of awakening, the relative area of spine profiles contacted by MFT reached similar levels to those estimated in active European hamsters (Table 1). The relative percentage area of MFT occupied by mitochondrial profiles was increased in hibernating compared with active hamsters and this increase persisted 3 h after deliberately awakening them from hibernation (Table 1). Whereas the MFT of active hamsters showed the typical rounded spine heads piercing the bouton surface at multiple sites, the spines contacted by MFT of hibernating hamsters appeared smaller, flattened and most of the time restricted to the periphery of the bouton (Fig. 4). Whereas these spines still bear asymmetric active synaptic zones during deep hypothermia, their postsynaptic densities (PSD) appear much thinner than those of active and awakened hamsters (average PSD thickness: 33.82 ± 2.49 nm vs. 46.90 ± 2.01 nm and 44.34 ± 2.47 nm; $P < 0.01$ and $P < 0.05$, compared with active and awakened animals, respectively, one-way ANOVA, Tukey post hoc test). We also observed an apparent dispersion of the small clear synaptic vesicle population in MFT during deep hypother-

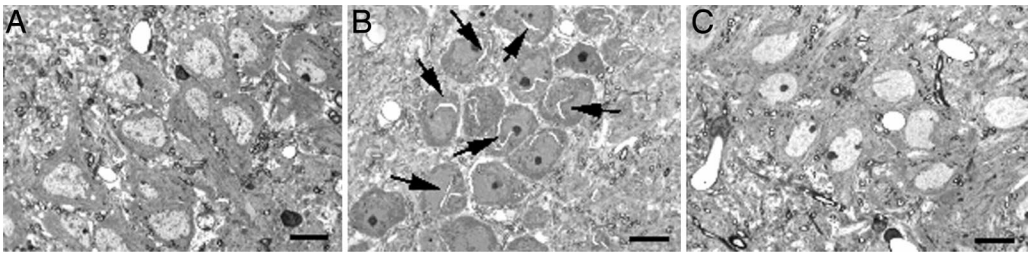

Fig. 3. Deep hibernation causes morphological changes in hippocampal CA3 pyramidal cell bodies. (*B*) Toluidine blue staining shows cytoplasmic slits (arrows) during hibernation bout. (*A* and *C*) No cytoplasmic slits were observed in cell bodies of active (*A*) or awakened (*C*) hamsters.

mia that reversed itself when euthermia was reached. There was a significant decrease in the estimated average density of clear small vesicles within MFT profiles of torpid hamsters (2,281.07 ± 56.63 vesicles per μm^3) compared with active and awakened animals (3,187.56 ± 63.89 and 3,206.75 ± 181.68 vesicles per μm^3, respectively; $P < 0.001$, one-way ANOVA, Tukey post hoc test).

Discussion

Dynamic Morphological Changes in Hippocampus Occur During the Hibernation Cycle. We report that the hippocampus of hibernating European hamsters undergoes a dynamic and reversible reorganization of the proximal and distal apical dendritic fields of CA3 pyramidal neurons. Whereas the architecture of the basal dendritic arborizations remained stable throughout the hibernation cycle, the simplification and retraction of the CA3 apical dendritic trees observed in hypothermic hamsters could be interpreted as an adaptive process to limit the powerful glutamatergic mossy fiber input they receive and limit the activation of the excitatory input from recurrent axonal collaterals that are known to project from neighboring CA3 pyramidal neurons (16, 17). These observations raise the possibility that the reversible changes in connectivity between the dentate gyrus and the CA3 hippocampal subregions associated with deep hypothermia could interfere with the processing and storage of information (13). In line with this notion, we find that hibernating European hamsters show a temporary loss of synaptic contacts between MFT and their postsynaptic complex spines that is restored only a few hours after inducing awakening. These results suggest that these morphological responses might mediate the disruption and reestablishment of the normal level of structural and functional connectivity within a key region of the brain during the transition between euthermia and hypothermia.

In addition to reversibly altering the morphology of nerve terminals and dendritic fields, we report that deep hibernation also affects the cytoplasm of CA3 pyramidal cell bodies, inducing the formation of characteristic slits associated with widened endoplasmic reticulum membranes. A recent report (18) described similar cytoplasmic slits in neuronal and nonneuronal tissues of deeply hypothermic ground squirrels. Freeze-fracture electron microscopic studies revealed that the slits are cross-sections of protein-free membrane patches that result from the lipid segregation and the displacement and exclusion of proteins induced by low temperature (18).

Our observations documenting that only a few hours after the induction of awakening are sufficient to reverse the hippocampal dendritic retraction, spine density and MFT reorganization during deep hibernation bouts are in agreement with previous reports (19, 20) describing a similar hippocampal remodeling during the hibernation cycle of another hibernating species, the Siberian ground squirrel. These observations suggest that the structural specializations detected in the hippocampus of hibernating animals have a more general evolutionary significance in response to unfavorable environmental conditions. Furthermore, both Popov *et al.* (19) and the present report show that the dendritic regrowth and axonal remodeling occur even during spontaneous active states when the animals rewarm for approximately a day or so between bouts of deep hypothermia (ref. 19 and this work). Taken together, our results and those on ground squirrels indicate a remarkably dynamic hippocampal structure and connectivity during the course of hibernation. In addition, they suggest that the rapid restoration of interneuronal connectivity and postsynaptic dendritic complexity upon rewarming and full resumption of brain electrical activity, may be use-dependent. Further support for the reversible hippocampal plasticity observed during the hibernation cycle is provided by the reversible formation and degradation of hyperphosphorylated forms of the cytoskeletal protein tau in the hippocampus of hibernating European ground squirrels (21). During torpor, hyperphosphorylated tau is particularly abundant in the CA3

Table 1. Effect of hibernation on the relative area of stratum lucidum occupied by MFT and the relative area of MFT occupied by giant spine and mitochondrial profiles

Morphological parameter	Active	Hibernating	Awake
% area MFT/SL	15.28 ± 1.29	16.51 ± 1.01	15.23 ± 0.57
% area spines/MFT	19.52 ± 1.82	11.08 ± 0.71*	17.52 ± 1.13
% area mit/MFT	3.75 ± 0.35	5.02 ± 0.22**	5.17 ± 0.34**

SL, stratum lucidum; mit, mitochondrial. *, $P < 0.001$ compared with hibernating and awake groups. **, $P < 0.05$, compared with active group, one-way ANOVA, Tukey post hoc test. Values are mean ± SEM.

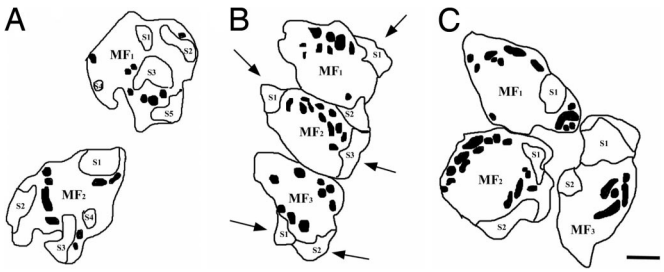

Fig. 4. Effect of deep hibernation and induced awakening on the morphology of MFT of European hamsters. Tracings of the boutons, spines, and mitochondrial profiles are depicted. (*A*) MFT of active hamsters are perforated by giant spine profiles from CA3 proximal apical dendrites where asymmetric synaptic contacts are found. (*B*) MFT of hibernating hamsters show a decrease in the percentage area occupied by spine head profiles compared with active controls. Note flattened spines restricted to the periphery of MFT (black arrows) and the increased percentage area occupied by mitochondrial profiles is depicted in black. (*C*) MFT of awakened hamsters show an ultrastructure similar to awake controls except for the increased percentage area occupied by mitochondrial profiles, depicted in black. MF, mossy fiber terminal; S, spine head. (Scale bar: 1 μm.)

subregion of the hippocampus and is not associated with the formation of pathological neurofibrillar aggregations, suggesting an intriguing and yet not fully understood physiological role in structural plasticity (21).

Dynamic Nature of MFT and Synaptic Contacts. One feature of the morphological remodeling of the mossy fiber-CA3 system of the European hamster hippocampus is the reorganized structure of the MFT during hibernation and arousal. What is particularly noteworthy is that hibernation alters the architecture of active synaptic zones between MFT and the giant apical dendritic spines known as thorny excrescences. The fact that CA3 hippocampal neurons in the brain of European hamsters rapidly restore the integrity of their apical dendritic arborizations and afferent MFT suggests a temporary, partial, and reversible disconnection between the dentate gyrus and the CA3 pyramidal neurons that could interfere with the processing of incoming information.

Another aspect of the hibernation-related morphological changes in the hippocampus is the dispersion of synaptic vesicles within MFT. We have reported a similar observation in rats with elevated corticosterone levels (22) and unpublished observations suggest that mice with the deletion of synapsin I and II also show dispersion and depletion of synaptic vesicles within MFT (A.M.M., V. Pieribone, B.S.M., and P. Greengard, unpublished data). In contrast, chronic stress in nonhibernating species such as the rat and mice is known to increase the packing density of synaptic vesicles in MFT (ref. 9; A.M.M. and B.S.M., unpublished observations). Although HPA activation and increase in glucocorticoid release has been linked to the arousal process (23), in the present work, we were unable to monitor glucocorticoid levels during the hibernation cycle simply because the placement of indwelling catheters for blood sampling prevented animals from hibernating (M.S. and P.P., unpublished observations). Nevertheless, we would suggest that decreased packing of synaptic vesicles may reflect elevated glucocorticoid levels and reduced synaptic activity. This latter suggestion is based on the finding noted above that the postsynaptic densities associated with the active zones between MFT and CA3 thorny excrescences appear significantly thinner in hibernating hamsters compared with active or awakened ones.

Hibernation Is Not Just a Passive State of Lesser Metabolic Activity. There is one intriguing aspect of the morphological changes reported in the present study that differs from the pattern of down-regulation during hibernation and reversal upon awakening. That is, the percentage area of mitochondrial profiles within MFT was increased compared with active animals. Furthermore, the percentage area of mitochondria in MFT of awakened hamsters was elevated even further when compared with hibernating hamsters, only to revert subsequently to normal levels in active European hamsters. Thus, not only is the awakening process a highly active resumption of euthermic metabolic activities, but also during hibernation itself, cellular activity is not simply arrested but, rather, a new metabolic set point is evidently established at a lower temperature.

There is evidence that this active process involves changes in protein synthesis and degradation and increased use of fat stores by mitochondria. For example, protein synthesis in the brain of hibernating ground squirrels is arrested by an active regulation that involves inhibition of protein initiation and elongation (24). Moreover, during hibernation, protein degradation is shut off by a process that is similar to that found in invertebrate quiescence where a ubiquitin-mediated proteolytic pathway is acutely blocked, preserving macromolecular integrity and providing tolerance to oxygen deprivation (25).

Another example of active regulation during hibernation is the finding that genes encoding pancreatic lipase and pyruvate dehydrogenase kinase isozyme 4 (PDK-4) are up-regulated in the heart of hibernating ground squirrels. PDK-4 prevents carbohydrate catabolism, and the resulting anaerobic glycolysis generates substrates for gluconeogenesis such as lactate (26). Fatty acids mobilized from adipose tissue are transported to the heart, where they are stored as mitochondrial-associated triglyceride droplets. Lipolysis by phospholipases provides a steady release of fatty acids at low temperatures, supplying substrate for mitochondrial beta-oxidation and the generation of ATP by oxidative phosphorylation (27, 28). These results provide support to the notion that physiological adaptations that take place during hibernation are controlled by differential genetic expression (2).

Role of the Hippocampus as a Dynamic Brain Structure That Adapts to Changing Environments. Hibernation represents a successful strategy for survival that involves disruption of the normal activities of food seeking, storage, and retrieval during times of scarce food supply. For animals living in seasonal environments, the shortening of day lengths is an accurate predictor of a change in food availability and imposes adaptive changes in behavior during the winter months such as deferral of reproduction, migration, storage of food for retrieval, and hibernation (14).

Migration and food storage strategies rely heavily on the capacity of the animal to track spatial distributions and to learn new spatial relationships among known landmarks (29). In birds and mammals, this function is mainly mediated by the hippocampus (30). A direct correlation has been found between hippocampal size and spatial ability both for orientation during migration and for retrieving scattered stored food (14, 31). Furthermore, for some food-storing bird species, seasonal changes in hippocampal volume are accompanied by seasonal increases in neurogenesis, another form of hippocampal plasticity (32).

Seasonal changes in hippocampal function are widely expressed in rodent species, such as the montane vole and the deer mouse which, when exposed to an increased photoperiod, perform better in the Morris water maze, a hippocampal dependent spatial task (33). In humans, seasonal changes in spatial learning have been documented, and correlations with annual cycles of testosterone in men have been described (34). Furthermore, patients suffering from seasonal affective disorder show deficits in spatial cognition tasks (35).

In contrast to migration and food storage, hibernation involves not only major metabolic readjustments to allow animals to survive winter months on their own fat stores but also a reorganization of the same brain structure, the hippocampus, that provides the means for spatial navigation and episodic and declarative memory storage that is so important in the active life of animals in relation to finding food. Because hibernating species live in an environment that requires no processing of new spatial information, one might expect concurrent decreases in the allocation of brain space reserved for such processing.

In conclusion, during the course of hibernation, the connectivity of the hippocampal formation of European hamsters undergoes dynamic and reversible changes that are likely to underlie the temporary disuse of exploratory activity, spatial navigation, and episodic memory skills during deep hypothermia. Such a condition may reinforce that state of torpor and inactivity that is essential for survival during winter months and allow animals to use their own limited energy reserves.

Materials and Methods

Animals. Adult male European Hamsters (*Cricetus cricetus*) were caught in the countryside in the vicinity of Strasbourg (France) in March–April 1994, just when they started to arouse from hibernation. After capture, the animals were kept in individual cages with pellet food and water ad libitum in outdoor condi-

tions. The hibernation period started in October–November, and at this time of the year, the hamsters were transferred to a climatic room kept under a 8/16 h light/dark cycle and 7 ± 1°C (as in natural conditions in December). In these conditions, the bouts of hypothermia characteristic of the hibernation cycle are expressed regularly. The hibernation cycle was monitored by a continuous registration of the core body temperature through Minimitter thermosensitive transmitters implanted in the hamster's abdominal cavity under halothane anesthesia just before placing the hamster within the climatic room (Dataquest III data acquisition system). All experimental procedures were in accordance with the National Institutes of Health principles of laboratory animal care (36) and French national laws.

Experimental Treatment Groups. Before the beginning of the experiment, European hamsters had been in the climatic chamber for at least 1 month and had all expressed regular bouts of hypothermia followed by periodic spontaneous arousals during which the animals became euthermic and active. Animals were assigned to three experimental groups: (*i*) active hamsters (n = 6) with a normal body temperature (core body temperature: 37°C) during the hibernation period, (*ii*) hibernating hamsters (n = 6) in deep hypothermia (core body temperature: 8–9°C) for at least 36 h, and (*iii*) awakened hamsters (n = 12) that were disturbed from their torpor by gentle hand manipulation during 30 sec, a manipulation that induces an arousal similar to that observed normally, i.e., a progressive rapid increase in body temperature with the euthermic stage being reached within 2–3 h. Animals in this group were killed 2 (n = 6) or 3 (n = 6) h after starting the manipulation.

Golgi Staining Procedure. European hamsters were anesthetized with halothane and transcardially perfused with 100 ml of saline solution followed by 200 ml of a fixative containing 2% glutaraldehyde and 2% paraformaldehyde in 0.1 M phosphate buffer (PB; pH 7.4). Two hours after the perfusions, brains were removed from the skulls and stored in the fixative overnight at 4°C. Coronal sections (100-μm thick) through the dorsal hippocampus were cut on a Vibratome and washed in PB. For each brain, 4 sections were used for electron microscopy (see below), whereas the remaining 14 sections were processed according to a modified version of the "single" section Golgi impregnation procedure (37). Briefly, brain sections were incubated in 3% potassium dichromate in distilled water overnight. Rinsed sections were mounted onto plain slides and a coverslip was glued over the sections at the four corners. These slide assemblies were incubated in 1.5% silver nitrate in distilled water overnight in the dark. During the following day, the slide assemblies were dismantled, and sections were rinsed in distilled water and dehydrated in absolute ethanol. The sections then were cleared in Histoclear (Americlear), mounted onto gelatinized slides, and coverslipped under Permount (Fisher Scientific).

Data Analysis of Golgi Material. ***Estimation of dendritic branching points and total length.*** Slides containing the Golgi-impregnated brain sections were coded before the analysis; the code was not broken until the analysis was complete. In addition to hippocampal CA3 pyramidal neurons, pyramidal neurons from layer V of parietal cortex also were examined for comparison purposes. Both the dorsal hippocampus and the parietal cortex examined in this study were contained in the same sections and, therefore, both brain regions were subjected to the same histological procedures. To be selected for analysis, Golgi impregnated pyramidal neurons had to possess the following characteristics. (*i*) The first is the location in layer V of parietal cortex and in the segment of the CA3 subregion proximal to the dentate gyrus of the dorsal hippocampus. The CA3 segment examined excluded the CA3 curvature and ended at the imaginary line connecting the ends of the dorsal and ventral blades of the dentate gyrus. This CA3 segment contains characteristic pyramidal neurons with well defined apical and basal dendritic trees and is devoid of the atypical and more heterogeneous pyramidal cell types mainly observed between the blades of the dentate gyrus. (*ii*) Cell bodies had to be located in the middle third of the tissue section to avoid analysis of impregnated neurons which extended largely into other sections. This last condition is crucial to achieve a consistent analysis and to ensure that all selected neurons are contained within the section thickness. Thus, we excluded from the analysis those superficially located neurons with cut-off processes that otherwise would have contributed to misleading underestimates: (*iii*) dark and consistent impregnation throughout the extent of all of the dendrites and (*iv*) relative isolation from neighboring impregnated cells that could interfere with analysis. Because the hippocampal subregion contains three well defined subtypes of pyramidal neurons (neurons with one primary shaft, short or long, and neurons with more than one primary shaft) with different degrees of apical branching patterns (38), special care was taken to include the same number of pyramidal neuron subtypes across experimental animals and experimental groups. For each brain and, therefore, for each experimental animal, 14 to 16 pyramidal cells from layer V of parietal cortex or hippocampal CA3 subregion were selected from both hemispheres. We were able to match neuronal subtypes across the hippocampi of the six experimental animals per group, resulting in the analysis of 84–96 neurons per experimental treatment. Each selected neuron was traced at a final magnification of ×560 on a digitizing tablet by using a Zeiss light microscope with a camera lucida drawing tube attachment. From these drawings, the number of dendritic branch points in both the basal and apical dendritic trees was determined for each neuron. In addition, the 2D length of the dendrites was estimated for each basal and apical dendritic tree from the tracings on the digitizing tablet by using ZIDAS (Zeiss Interactive Digitizing Analysis System; Carl Zeiss, Thornwood, NY).

Estimation of dendritic branching density. Because the Golgi analysis detected differences only in the branching pattern and length of the apical and not the basal dentritic trees, the branching density of the apical dendritic trees of CA3 pyramidal neurons of active, hibernating, and awaken hamsters (3 h) was evaluated by using a variation of the Sholl method (39, 40). An acetate sheet containing a series of concentric circles calibrated at 20-μm intervals was superimposed to each tracing so that the center of the circles coincided with the center of the cell body. The number of intersections between the dendrites and the concentric circles was counted and plotted as a function of the distance from the soma.

Estimation of spine density. The analysis was performed on Golgi-impregnated brain sections containing the dorsal hippocampus of six hamsters per experimental group. The number of visible spines was counted on apical dendrites of CA1 and CA3 pyramidal neurons. The dendritic segments selected for analysis were sampled from lateral third-order dendrites located in the middle third of the stratum radiatum. All segments were relatively thin and of similar diameter to minimize the effect of hidden spines above or below the dendrite and to balance these effects among different cells. Dendritic segments had to remain in a single plane of focus so that the length of the dendrite projected in 2D would approximate the 3D dendritic length. Dendritic segments were traced with the aid of a camera lucida drawing tube at ×1,400, and the length of each segment was measured from the tracings on a digitizing tablet (ZIDAS). Five dendritic segments, at least 15 μm in length, were analyzed per neuron, and 12 neurons were analyzed per experimental animal. Data were expressed as number of spines per micrometer of dendrite.

Statistical analysis. Means were determined for the number of branch points, total dendritic length, dendritic intersections per circle for each brain, and a final average was calculated per experimental group. For spine-density estimations, the average of the number of spines per micrometer was calculated per neuron and per animal, and then a final average was calculated per experimental group. Group differences were tested by using one-way analysis of variance followed by Tukey honestly significantly different post hoc comparisons. A probability level of $P < 0.05$ was used as the criterion for statistical significance.

Electron microscopy. Sections containing the same anteroposterior level of the dorsal hippocampus from six European hamsters per experimental condition were rinsed in PB and postfixed in 2% osmium tetroxide in PB for 2 h, rinsed, and partially dehydrated through an ascending series of ethanol (50% and 70%). Sections were stained with 2% uranyl acetate in 70% ethanol and further dehydrated with 95% and 100% ethanol. Ethanol then was replaced with propylene oxide, and sections were flat embedded in Durcupan (Fluka, Buchs, Switzerland). The mossy fiber termination zone (stratum lucidum) was trimmed, and ultrathin silver sections were cut on a Reichterdt ultramicrotome and mounted on single-slot copper grids coated with formvar film. Sections were counterstained with Reynolds' lead citrate, and the final preparations were examined and photographed with a Jeol 100 CX electron microscope. Photographs (10 per subject) were randomly taken from the stratum lucidum covering an area of 1.3 mm^2 at a primary magnification of $\times$5,400. Prints at a final magnification of $\times$13,500 were used to trace MFT and the embedded mitochondria and giant spine profiles. Between 45 and 50 MFT per experimental animal were analyzed (and a total of 270–300 MFT per experimental group).

Data analysis. The area of MFT profiles and the areas occupied by embedded mitochondria and spine profiles relative to the stratum lucidum area surveyed were estimated with the aid of the ZIDAS system. Synaptic vesicle density was estimated by using the intersection method, positioning an unbiased counting frame with squares of known area (0.2 cm^2) at the coordinates of a quadratic lattice superimposed on the micrographs containing the MFT. The number of vesicles per unit area was extrapolated to the number of vesicles per unit volume by using a variation of Floderus equation (ref. 41; see ref. 15 for details). Each variable was averaged across MFT to obtain a single mean value per animal, one-way ANOVA analysis was performed and statistical significance was considered at $P < 0.05$.

We thank Dr. Alison North for taking the picture of the Golgi-impregnated neuron. This work was supported by National Institutes of Health Grant MH 41256 (to B.S.M.), Servier (France), and The Health Foundation (New York).

1. Lyman CP, Chatfield PO (1955) *Physiol Rev* 35:403–425.
2. Boyer BB, Barnes BM (1999) *BioScience* 49:713–723.
3. Beckman AL, Stanton TL (1982) in *The Neural Basis of Behavior*, ed Beckman AL (Spectrum Publications, New York), pp 19–46.
4. Lyman C, Willis J, Malan A, Wang L (1982) *Hibernation and Torpor in Mammals and Birds* (Academic, New York).
5. Hermès MLHJ, Buijs RM, Masson-Pévet M, Van der Woude T, Brenklé R, Kirsch R, Pévet P (1989) *Proc Natl Acad Sci USA* 86:6408–6411.
6. Dubois-Dauphin M, Theler JM, Zagamidis N, Domonik W, Tribollet E, Pévet P, Charpak G, Dreifuss JJ (1991) *Proc Natl Acad Sci USA* 88:11163–11167.
7. Hermès, MLHJ, Kalsbeek A, Kirsch R, Buijs RM, Pévet P (1993) *Brain Res* 631:313–316.
8. Pévet P, Masson-Pévet M, Hèrmes MLHJ, Buijs RM, Ganguilhem B (1989) in *Living in the Cold II*, eds Malan A, Ganguilhem B (Libbey, London), pp 43–51.
9. McEwen BS, Magariños AM (1997) *Ann NY Acad Sci* 821:271–284.
10. Pakhotin PI, Pakhotina ID, Belousov AB (1993) *Prog Neurobiol* 40:123–161.
11. South FE, Heath JE, Luecke RH, Mihailovic LT, Myers RD Panuska JA, Williams BA, Hartner WC, Jacobs HK (1972) in *Hibernation and Hypothermia, Perspectives and Challenges*, eds South FE, Hannon JP, Willis JR, Pengelley ET, Alpert NR, (Elsevier, Amsterdam), pp 629–633.
12. Igelmund P, Spangenberger H, Nikmanesh FG, Gabriel A, Lütke K, Zhao YQ, Böhm-Pinger MM, Heinemann U, Hescheler J, Klussmann FW (1996) in *Adaptations to the Cold: Tenth International Hibernation Symposium*, eds Heiser F, Hulbert AJ, Nicol SC (Univ of New England Press, Armidale, Australia), pp 159–166.
13. Eichenbaum H (1997) *Science* 277:330–332.
14. Jacobs LF (1996) *Biol Bull* 191:92–100.
15. Magariños AM, García Verdugo J, McEwen BM (1997) *Proc Natl Acad Sci USA* 94:14002–14008.
16. Li XG, Somogy P, Ylinen A, Buzsaki G (1994) *J Comp Neurol* 339:181–208.
17. Gomez di Cesare CM, Smith KL, Rice FL, Swann JW (1997) *J Comp Neurol* 384:165–180.
18. Azzam NA, Hallenbeck JM, Kachar B (2000) *Nature* 407:317–318.
19. Popov VI, Bocharova LS, Bragin AG (1992) *Neuroscience* 48:45–51.
20. Popov VI, Bocharova LS (1992) *Neuroscience* 48:53–62.
21. Arendt T, Stieler J, Strijkstra AM, Hut RA, Rüdiger J, Van der Zee EA, Harkany T, Holzer M, Härtig W (2003) *J Neurosci* 23:6972–6981.
22. Magariños AM, Orchinik M, McEwen BS (1998) *Brain Res* 809:314–318.
23. Mussachia XJ, Deavers DR (1981) in *Survival in the Cold*, eds Musacchia XJ, Jansky L (Elsevier North–Holland, Amsterdam), pp 13–32.
24. Frerichs KU, Smith CB, Brenner M, De Grazia DJ, Krause GS, Marrone L, Dever TE, Hallenbeck JM (1998) *Proc Natl Acad Sci USA* 95:14511–14516.
25. Anchordoguy TJ, Hand SC (1994) *Am J Physiol* 267:R895–R900.
26. Galster W, Morrison PR (1975) *Am J Physiol* 228:325–330.
27. Burlington RF, Bowers WD, Jr, Daum RC, Ashbaugh P (1972) *Cryobiology* 9:224–228.
28. Andrews MT, Squire TL, Bowen CM, Rollins MB (1998) *Proc Natl Acad Sci USA* 95:8392–8397.
30. Bingman VP (1990) in *Neurobiology of Comparative Cognition*, ed Olton DS (Lawrence Erlbaum, Hillsdale, NJ), pp 423–447.
31. Sherry DF, Forbes MRL, Khurgel M, Ivy GO (1993) *Proc Natl Acad Sci USA* 90:7839–7843.
32. Barnea A, Nottebohn F (1994) *Proc Natl Acad Sci USA* 91:11217–11221.
33. Galea LA, Kavaliers M, Ossenkopp KP, Innes D, Hargreaves EL (1994) *Brain Res* 635:18–26.
34. Kimura D, Hampson E (1994) *Curr Dir Psychol Sci* 3:57–61.
35. O'Brien JT, Sahakien BJ, Checkley SA (1993) *Br J Psychiatry* 163:338–343.
36. Committee on Care and Use of Laboratory Animals (1985) *Guide for the Care and Use of Laboratory Animals* (Natl Inst Health, Bethesda), DHEW Publ No (NIH) 85-23.
37. Gabbot PL, Somogyi J (1984) *J Neurosci Meth* 11:221–230.
38. Fitch JM, Juraska JM, Washington LW (1989) *Brain Res* 479:105–114.
39. Sholl DA (1956) *J Anat* 87:387–406.
40. Uylings HBM, Ruiz-Marcors A, van Pelt J (1986) *J Neurosci Methods* 16:127–151.
41. Pierce JP, Mendell LM (1993) *J Neurosci* 13:4748–4763.